Journal of Alloys and Compounds 633 (2015) 323–328

Contents lists available at ScienceDirect

Journal of Alloys and Compounds

journal homepage: www.elsevier.com/locate/jalcom

Preparation of $Cu–Al_2O_3$ bulk nano-composites by combining Cu–Al alloy sheets internal oxidation with hot extrusion

Fengzhang Ren [a,b,*], Aijuan Zhi [c], Danwen Zhang [a], Baohong Tian [a], Alex A. Volinsky [d], Xiaoni Shen [a]

[a] School of Materials Science and Engineering, Henan University of Science and Technology, Luoyang 471023, China
[b] Henan Collaborative Innovation Centre of Non-Ferrous Generic Technology, Luoyang 471023, China
[c] College of Information Technology, Luoyang Normal University, Luoyang 471022, China
[d] Department of Mechanical Engineering, University of South Florida, Tampa, FL 33620, USA

ARTICLE INFO

Article history:
Received 16 November 2014
Received in revised form 22 January 2015
Accepted 6 February 2015
Available online 14 February 2015

Keywords:
$Cu–Al_2O_3$ nano-composites
Bulk materials
Internal oxidation
Hot extrusion
Microstructure
Properties

ABSTRACT

$Cu–Al_2O_3$ bulk nano-composites were prepared by combining Cu–Al alloy sheets internal oxidation with hot extrusion. Cu–0.16 wt.%Al alloy sheets, 90 mm in diameter and 0.5 mm thick were internally oxidized with $Cu_2O + Cu + Al_2O_3$ mixed powders at 900 °C for 8 h. Nano-sized Al_2O_3 particles were distributed in the Cu matrix with a coherent interface. The orientation relationship between the Cu matrix and the Al_2O_3 particle was $[2\ 1\ \bar{1}]_{Cu}//[\bar{1}\ 1\ 0]_{Al2O3}$, $(0\,2\,2)_{Cu}//(2\,2\,0)_{Al2O3}$ and $(1\ \bar{1}\ 1)_{Cu}//(0\ 0\ \bar{2})_{Al2O3}$. Oxidized sheets were cleaned, stacked, vacuum sealed and hot extruded at 800 °C to prepare $Cu–Al_2O_3$ nano-composite rods with a 20 mm diameter. The $Cu–Al_2O_3$ rods were cold drawn to a wire with a diameter of 3 mm. The hot extruded rod and the cold drawn wire cross-sections presented concentric rings features, resembling tree rings. In the rings structure, the closer to the edge of the rod or the wire, the thinner the $Cu–Al_2O_3$ sheets were with better interfacial bonding. The electrical conductivity of the rod was 96.3% IACS (International Annealed Copper Standard). The electrical conductivity, yield strength, tensile strength and reduction of the cross-sectional area of the drawn wire were 94.1%IACS, 417 MPa, 445 MPa and 80.2%, respectively. The paper demonstrates a feasible way to prepare $Cu–Al_2O_3$ bulk nano-composites.

1. Introduction

Dispersion strengthened copper alloy is a kind of copper matrix composite made by introducing fine dispersion particles as the strengthening phase in the copper matrix [1,2]. Due to the high thermal and electrical conductivity, along with high strength and excellent high temperature resistance, these materials have become a research focus in the field of copper matrix composites [3–5]. Currently, the internal oxidation is a popular method to prepare the dispersion strengthened copper alloys with more homogeneous microstructure. It can be further divided into powder internal oxidation and layer internal oxidation methods [6].

The common procedure of the powder internal oxidation is as follows: Preparation of the copper-based solid solution alloy powder → mixing the alloy and oxidizer powders → internal oxidation → deoxidizing treatment → mold pressing → sintering process → plastic deformation [7]. The powder internal oxidation method requires powder atomizing and vacuum sintering equipment [8–10], resulting in high equipment cost, only suitable for the high volume production.

During the layer internal oxidation process a sheet or a rod of the copper-based solid solution alloy is packed in the oxidizer and then heated for internal oxidation. This process results in the formation of the dispersion strengthened copper alloy layer near the surface of a sheet or a rod (for a sheet, it can be fully oxidized) [11,12]. The layer internal oxidation can be easily achieved and does not require expensive equipment. However, at present it is only applied to prepare thin layers of the dispersion strengthened copper alloy. It is most commonly used to prepare thin sheets of the dispersion strengthened copper alloy, since the solid solution alloy sheet can be fully oxidized [6]. Research on how to use the fully oxidized solid solution alloy sheet to prepare bulk dispersion strengthened copper alloy is rare. A common copper alloy for the internal oxidation is the Cu–Al alloy. Zhang et al. [13] (our research team members) have used hot press forming for the oxidized Cu–Al alloy sheets to prepare small $Cu–Al_2O_3$ composite bulk samples, but the tensile strength was relatively low at 200 MPa. Thus,

---

[*] Corresponding author at: School of Materials Science and Engineering, Henan University of Science and Technology, Luoyang 471023, China. Tel.: +86 379 64231846; fax: +86 379 64230597.

E-mail addresses: renfz@haust.edu.cn, lyrenfz@163.com (F. Ren).

http://dx.doi.org/10.1016/j.jallcom.2015.02.057
0925-8388/

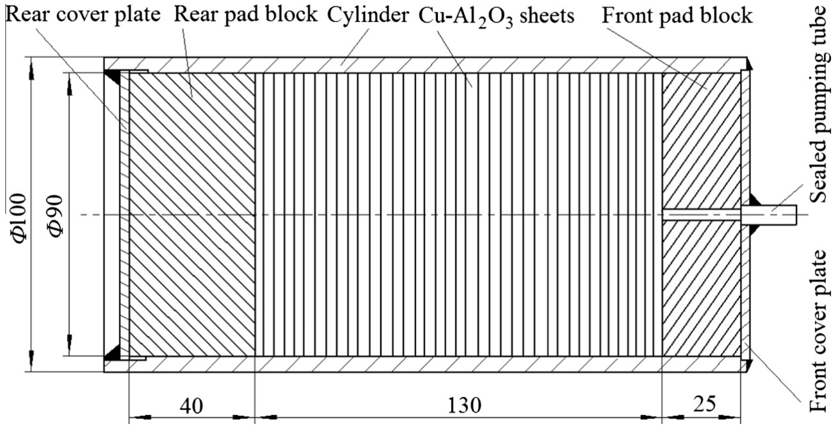

Fig. 1. Schematic of the hot extrusion vacuum package.

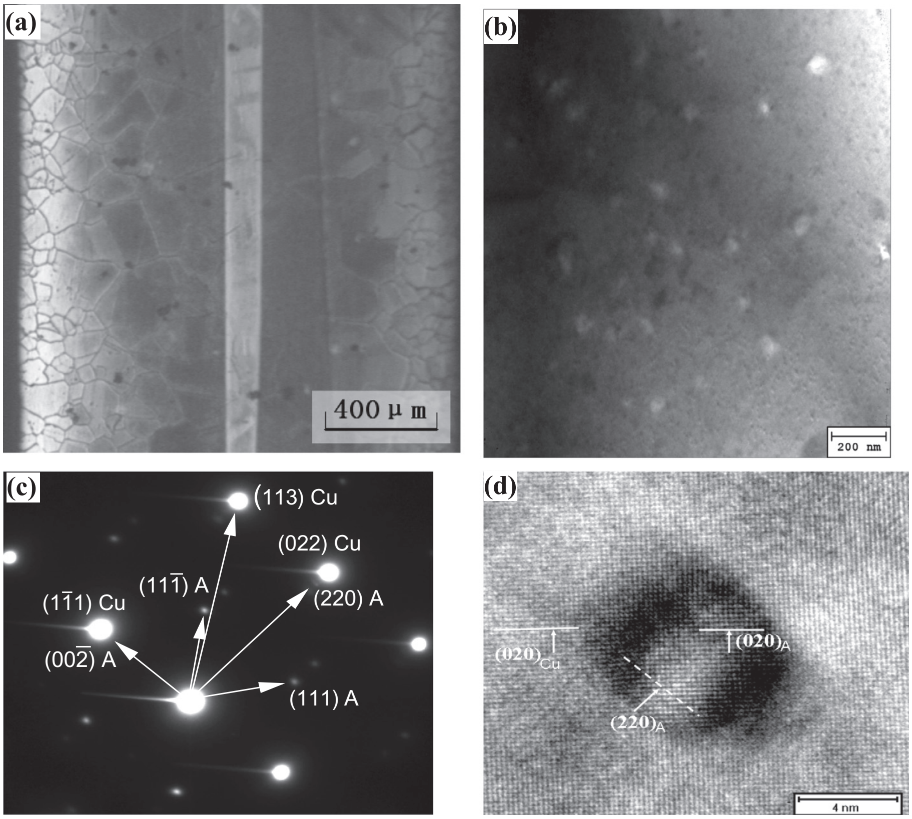

Fig. 2. Microstructure of the Cu–0.16 wt.%Al alloy sheets after internal oxidation (a) internal oxidation layers at both sides and the un-oxidized layer in the middle; (b) Al_2O_3 nanoparticles precipitation in the Cu matrix; (c) SAED pattern and indexed results of the SAED pattern; (d) coherent interface between Al_2O_3 particle and Cu matrix (in (c) and (d), A denotes Al_2O_3).

preparation of bulk dispersion strengthened copper alloy by Cu–Al alloy sheet internal oxidation needs to be further studied. Moreover, there are different perceptions for the type of precipitated Al_2O_3 [9] and the interface characteristics between Cu matrix and Al_2O_3 particle are seldom studied.

This paper aims to explore a new method of bulk dispersion strengthened copper alloy preparation. Cu–Al_2O_3 bulk composite rod was prepared by combining Cu–Al alloy sheets internal oxidation with hot extrusion. The structure and properties of hot extrusion rod and its drawn wire (a trial product) were studied. The interface characteristics between the Cu matrix and the Al_2O_3 particle in the internal oxide layer of the oxidized sheet were also investigated.

2. Experimental details

2.1. Preparation of the Cu–Al_2O_3 bulk composites (rod and wire)

2.1.1. Smelting of Cu–Al alloy and internal oxidation of Cu–Al alloy sheets

The raw materials used were commercial electrolytic copper (⩾99.99 wt.% pure) and industrial aluminum (⩾99.9 wt.% pure). Raw copper and aluminum (0.16 wt.% theoretical aluminum content) were melted in a graphite crucible placed in a medium-frequency induction furnace under open atmosphere. The molten

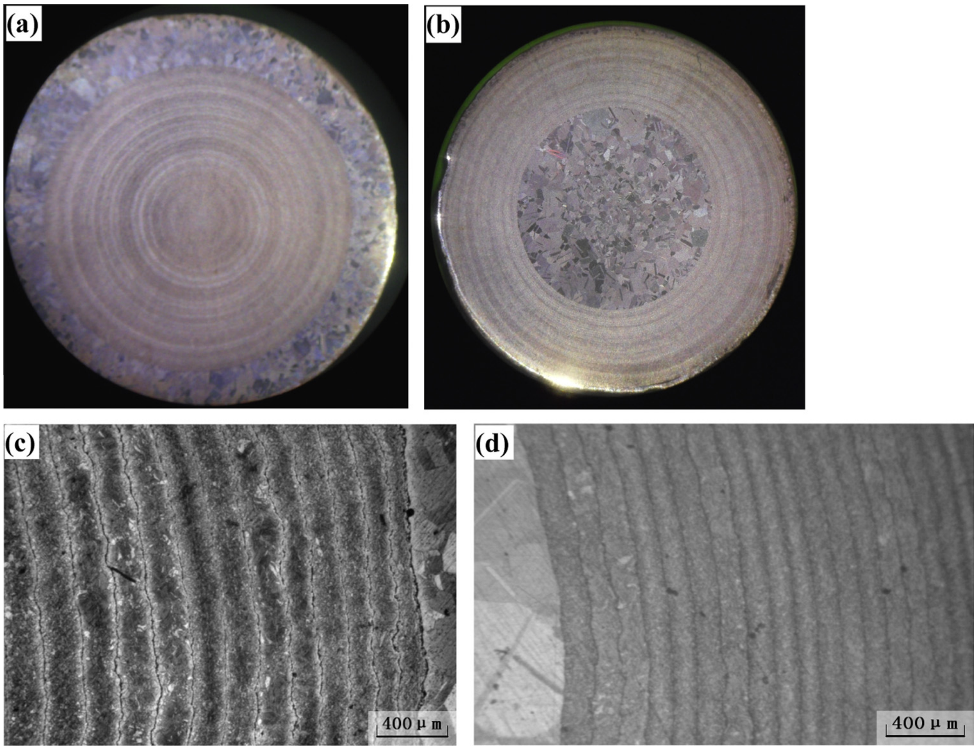

Fig. 3. Morphology of the cross-section of the hot extrusion rod (a) and (b) macrostructure of the cross-section at 0.5 m from the front end and 1 m from the rear end, respectively (∅20 mm); (c) and (d) microstructure of the Cu–Al_2O_3 composites at 0.5 m from the front end and 1 m from the rear end.

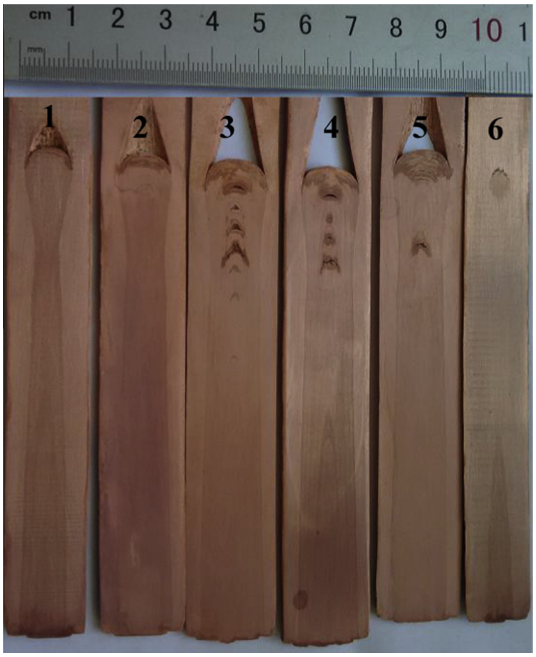

Fig. 4. Axis profile of the extrusion rod at the front end.

alloy was poured in the cast steel mold. The size of the Cu–Al alloy ingot was ∅80 mm × 150 mm, and totally 3 pieces were made. The ingot composition analysis showed that the Al content of the ingot was the same as before smelting, which indicated that the Al was not oxidized during smelting.

After removing the outer skin of the ingot, it was forged to a billet with a rectangular cross-section of 12 × 40 mm^2 (the forging temperature was 750–850 °C), and then multi-pass cold-rolled and intermediately annealed many times. The recrystallization annealing temperature was 450 °C and the holding time was 1.5 h. Annealing was performed every time the thickness was reduced by about 30%. It was ultimately rolled into a sheet with a thickness of 0.5 mm and a width of about 92 mm. The rolled sheet was cut into about 100 round circular sheets with 90 mm diameter. The round sheets were mechanically polished and oil was washed off by hot aqueous alkali and acetone.

The round alloy sheets were buried in a mixed powder within a welded copper pot. There must be powder between any two sheets so that they would not come in close contact with each other. A metallographic 1.5 mm thick sample was cut from the same forged billet and also buried in the powder. The thicker sample was used to conveniently observe the internal oxidation layer. The mixed powder was 30 wt.% Cu_2O (⩽100 μm) + 20 wt.% Cu (⩽74 μm) + 50 wt.% Al_2O_3 (⩽50 μm). Cu and Cu_2O powders were added to ensure adequate oxygen partial pressure for internal oxidation of the Cu–Al alloy. The problem of oxygen partial pressure during internal oxidation has been studied in many reports [7,10,14]. Al_2O_3 powder was added to prevent sheets from bonding with Cu and Cu_2O powders during internal oxidation. After the alloy sheets and the metallographic sample were buried in the mixed powder, the copper pot was covered with copper lid and then the gap between the pot and the lid was sealed with the refractory slurry (mixture of refractory clay and sodium silicate in the 1:2 mass ratio). The sealed pot was placed in the resistance furnace to carry out internal oxidation at 900 °C for 8 h. According to the past experience, under these internal oxidation conditions, the sheets with a thickness of 0.5 mm should be fully oxidized. This can be verified by observing the metallographic sample using optical microscopy. After the internal oxidation, Cu–0.16 wt.%Al alloy sheets became Cu–0.30 wt.%Al_2O_3 composite sheets. The microstructure of the Cu–0.30 wt.%Al_2O_3 composite was further observed by JEM-2100 high resolution transmission electron microscopy (HRTEM). The round composite sheets were similarly treated with mechanical polishing and washing off oil by hot aqueous alkali and acetone.

2.1.2. Cu–Al_2O_3 sheets sealing and hot extrusion

The Cu–0.30 wt.%Al_2O_3 composite sheets were stacked in a cylinder, vacuum-sealed, and then hot extruded to prepare the Cu–Al_2O_3 bulk composites. The purpose of vacuum sealing was to prevent the sheets surface from oxidation during hot extrusion, since surface oxidation affects the interfacial bond strength between the sheets. The vacuum sealing procedure was as follows: (1) The pumping tube, the front cover plate and the cylinder were welded together, as shown in Fig. 1. (2) The front pad block, stacked sheets, the rear pad block and the rear cover plate were placed in the cylinder and then compacted, followed by the rear cover plate welded onto the cylinder. All welded seams were gas-tight. (3) One end of the pumping tube was connected to a small custom-made three-way valve. The other two ends of the three-way valve were connected to a vacuum pump and an argon source. The package was repeatedly exposed to vacuum and filled with argon, and eventually under vacuum, the pumping tube was heated, hammer flattened to seal it and then cut off. The pumping tube was also seal-welded at the flat end to prevent cracking during heating, since the flat end cracking would result in air getting into the vacuum sealed package.

The cover plates, the cylinder, and the pad blocks were all made from the industrial pure copper. The size of the cylinder depended on the adopted extrusion die. The front and the rear pad blocks were mainly used to improve the utilization rate of the composite sheets and to coordinate the composite sheets deformation. Their thickness was only based on a simple analysis for plastic flow during extrusion and was not strictly controlled.

The vacuum package was heated at 800 °C for 2 h and then hot extruded into a rod with a diameter of 20 mm and a length of 4.9 m (sealed pumping tube was facing toward the extrusion outlet and was extruded first). The extrusion equipment used was a double-action 8 MN extruder. The preheating temperature of the extrusion die was 400 °C. The extrusion speed was 35 mm s^{-1} and the extrusion pressure was 780 MPa.

The intermediate section of the extrusion rod was cold drawn by multiple passes into a wire with a diameter of 3 mm (the trial product).

2.2. Structure and mechanical properties characterization

The macroscopic and microscopic structure of the cross-section at different locations of the hot extruded rod and drawn wire was characterized. The microstructure observations were carried out using the OLYMPUS PMG3 metallographic microscope. The electrical conductivity of the rod was measured using the Foerster SIGMATEST 2.069 eddy current conductivity meter, and the electrical conductivity of the wire was measured using the ZY9987 digital micro-ohmmeter. Tensile strength of the rod and the wire was measured using the Shimdzu AG-1250KN tensile testing machine, with the tension rate of 1 mm s^{-1}. The tensile specimen of the wire was directly cut from the wire and not machined. The tensile specimen of the hot extruded rod is described later in this article. The hardness of the composites was measured using the MH-3 microhardness tester. Load and hold time were 1.96 N (200 g) and 15 s, respectively. The mean value of the hardness was taken as an average of 5 measurements.

3. Experimental results and analysis

3.1. Cu–0.16 wt.%Al alloy sheets internal oxidation layer microstructure

The microstructure of the Cu–0.16 wt.%Al alloy metallographic sample with a thickness of 1.5 mm after internal oxidation at 900 °C for 8 h is shown in Fig. 2. The internal oxidation depth of the one side was 0.68 mm, thus the middle portion was not oxidized, as seen in Fig. 2(a). Thus, the Cu–0.16 wt.%Al alloy sheets 0.5 mm thick must be oxidized. Nano-Al_2O_3 particles were distributed in the Cu matrix in the internal oxide layer, as seen in Fig. 2(b). Fig. 2(c) is the selected area electron diffraction (SAED) pattern of the sample in Fig. 2(b), also showing indexed results of the SAED pattern (card number JCPDS75-0921, Al_2O_3, face centered cubic, lattice constant *a* = 0.395 nm). This Al_2O_3 is neither α-Al_2O_3 nor γ-Al_2O_3. The orientation relationship between the Cu matrix and the Al_2O_3 particle is $[2\ 1\ \bar{1}]_{Cu}//[\bar{1}\ 1\ 0]_{Al2O3}$, $(022)_{Cu}//(220)_{Al2O3}$ and $(1\ \bar{1}\ 1)_{Cu}//(0\ 0\ \bar{2})_{Al2O3}$. The lattice misfit between $(022)_{Cu}$ and $(220)_{Al2O3}$ is 8.86%, and that between $(1\ \bar{1}\ 1)_{Cu}$ and $(0\ 0\ \bar{2})_{Al2O3}$ is 5.51%. The interface between them is coherent, as shown in Fig. 2(d). Li et al. [15] investigated the microstructure and properties of the Cu–0.12 wt.%Al_2O_3 composite produced by internal oxidation after annealing at 900 °C. Their results showed that after annealing the composite hardness reduced by only 13%. During annealing the recovery occurred, while recrystallization did not occur in the composite, and the Al_2O_3 particles did not aggregate and grow. This indicates that the internally oxidized Cu–Al_2O_3 composite has excellent heat stability, and that the properties of the Cu–Al_2O_3 composite would not change after hot extrusion at 800 °C.

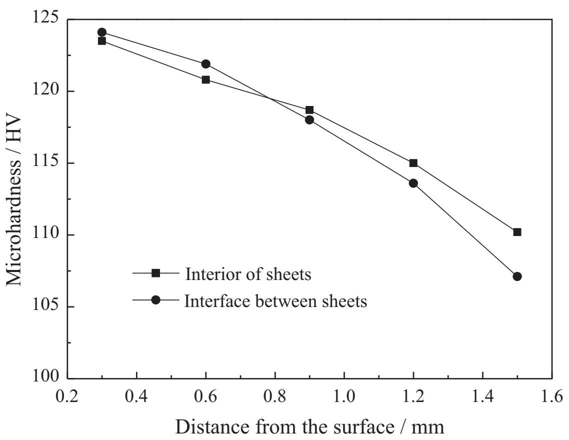

Fig. 5. Microhardness changes of the sheet interior and the interface as a function of the distance from the wire surface.

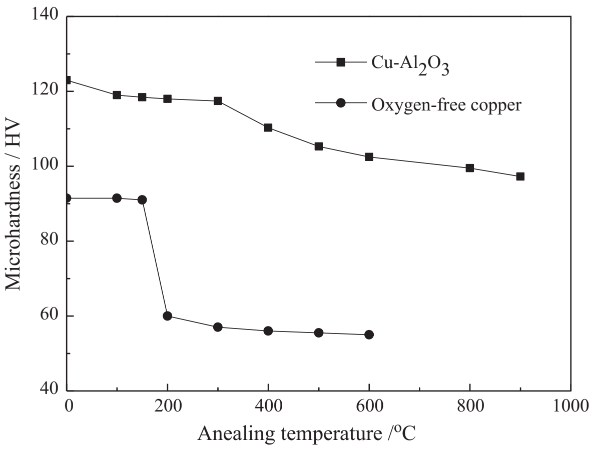

Fig. 6. Effects of annealing temperature on the surface microhardness of the cold-drawn Cu–Al_2O_3 bulk composites and strain hardening oxygen-free copper. Oxygen-free copper hardness data is from reference [14].

3.2. Cu–Al_2O_3 composite rod structure and properties

The macrostructure and the microstructure, respectively, of the cross-sections at 0.5 m from the front end (the end with the sealed pumping tube) and 1 m from the rear end of the hot extrusion rod are shown in Fig. 3. The center of the front portion of the hot extrusion rod is Cu–Al_2O_3 bulk composite with a diameter of 15 mm, wrapped with a 2.5 mm thick packaging layer, as seen in Fig. 3(a). The center of the back portion is formed of the packaging materials (11 mm in diameter), with 4 mm thick Cu–Al_2O_3 bulk composites outside with a very thin edge layer of the packaging materials (0.5 mm thick), forming a sandwich structure, as seen in Fig. 3(b). Cu–Al_2O_3 bulk composites have concentric rings structure both in the front and the back. In the ring structure, the closer to the edge, the thinner the Cu–Al_2O_3 sheets are and the better the Cu–Al_2O_3 sheets interfacial bonding is, as seen in Fig. 3(c) and (d). This also shows that during the hot extrusion, the deformation at different locations of the cross-section is different, less at the center and more at the edge. Cu–Al_2O_3 bulk composites of the front portion of the extrusion rod have a thick wrap layer of the packaging materials, while the back ones have a thick sandwich of the packaging materials, related to the design of the pad blocks. The problems of how to thin the front wrap layers and shorten the length of the back sandwich need to be further considered in the packaging design. According to the past experience, extrusion is difficult and the utilization rate of Cu–Al_2O_3 is low without the pad blocks.

A small portion, between 0.35 m and 0.5 m from the front end of the extrusion rod was cut along the extrusion rod axis into 6

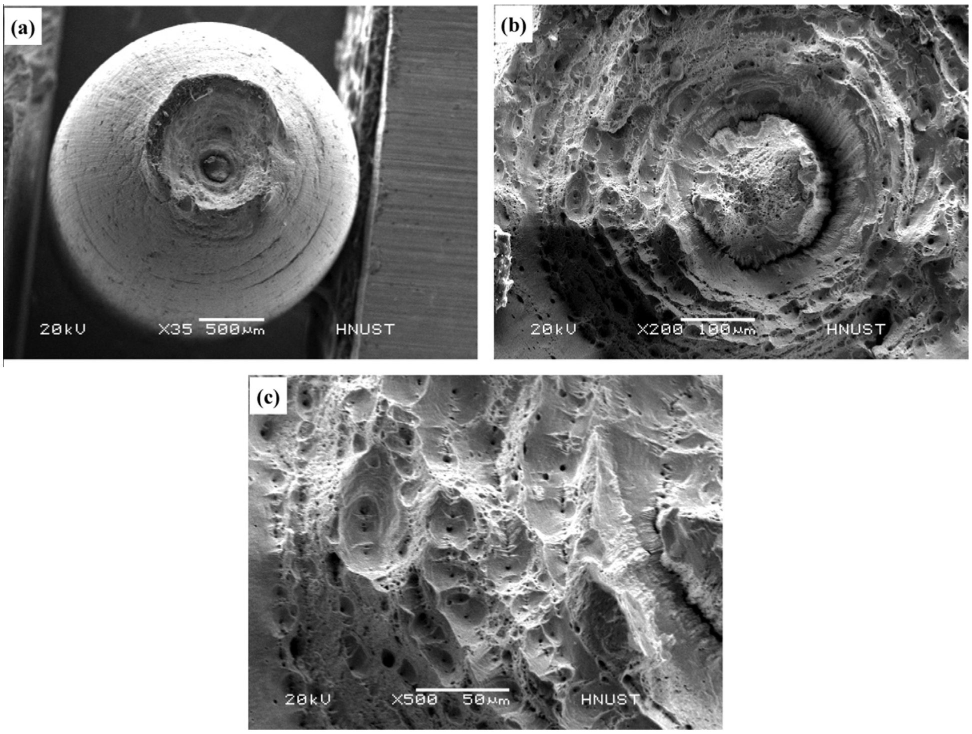

Fig. 7. Tensile fracture morphology of the cold-drawn Cu–Al_2O_3 composites (a) macro morphology; (b) micro fracture; (c) interface morphology.

plates by wire electrical discharge machining. The middle part of each plate is Cu–Al_2O_3 bulk composites, as shown in Fig. 4 (not strictly symmetrically cut). In Fig. 4, each section is sequentially numbered as No. 1–6, from left to right. It shows that the closer to the axes of the extrusion rod, the worst the interfacial bond between the Cu–Al_2O_3 composite sheets is (No. 3 and 4), which also shows that the deformation in the center of the extrusion rod is small. Meanwhile, the macro-defects of the bulk composites gradually decrease from front to back. The thickness of the middle 4 plates (No. 2–5) is 2.5 mm. No. 2, 4 and 5 were all machined into strip tensile specimens (tensile specimen was cut from the lower part with less defects). No. 3 was not suited for tensile testing because of many macro-defects. The cross-section size of the gauge part of the tensile specimen was 2.4 mm × 5.5 mm, and the gauge length was 40 mm (to ensure that the gauge portion is all Cu–Al_2O_3 bulk composites). In the gauge portion of each specimen, there are Cu–Al_2O_3 sheets interfaces approximately perpendicular to the tensile direction, resulting in interfacial fracture if the interfacial bonding is poor. The tensile strength of the samples No. 2, No. 4 and No. 5 is 332 MPa, 297 MPa and 321 MPa, respectively, and the percentage total elongation after fracture is 25.9%, 18% and 17.3%, respectively. The specimen farther away from the axis of the extrusion rod has a higher tensile strength.

The electrical conductivity of the ∅10 mm × 10 mm Cu–Al_2O_3 bulk composites cut from the extrusion rod (there is no packaging material in it) is up to 96.3%IACS.

3.3. Structure and properties of the cold-drawn wire

The 4.9 m long extruded rod was cut 0.5 m in the front and 1 m in the back. The remaining middle part of the hot extrusion rod was cleared off the outer wrappage (owing to the different thickness of the outer wrappage at different locations, the diameter of the cleared rod at different locations was different). The middle hot extrusion rod was multi-pass cold drawn to a wire with a diameter of ∅3 mm, 99 m long. The wire was divided into 12 sections, numbered No. 1–12 from the front to the end in sequence.

The cross-section microstructure of both ends of the samples No. 1–10 still has concentric rings, formed of the Cu–Al_2O_3 composites. These were used as a trial product (small part of No. 5 was used for mechanical properties testing), and their total length was 83 m. The cross section of the one end of the sample No. 11 and the cross sections of two ends of the sample No. 12 contained sandwich packaging material. Thus, samples No. 11 and 12 were discarded. It can be concluded that the center of the portion of the extruded rod, 0.5–3.4 m from the front of the extruded rod is formed of the Cu–Al_2O_3 composites.

The mean electrical conductivity of the wire samples No. 1–10 is 94.1% IACS, slightly lower compared with the conductivity of the extruded rod. The decrease of the electrical conductivity is due to the increase of the dislocation density after cold drawing, while dislocations increase electron scattering [16]. However, the wire electrical conductivity is still high enough.

Specimens for hardness and tensile testing were cut from the sample No. 5. In the ring structure of the wire, microhardness of the sheet interior and the interface as a function of the distance from the wire surface is shown in Fig. 5. From the surface to the center the microhardness decreases. This is because the deformation from the surface to the center decreases gradually during hot extrusion and cold drawing, resulting in better interfacial bonding near the surface and obvious strain hardening. In the center of the wire, the hardness of the sheet interior is higher than at the interface as a result of poor interfacial bonding and interfacial micro-defects.

Fig. 6 shows the effects of annealing temperature on the surface microhardness of the cold-drawn Cu–Al_2O_3 bulk composites and strain hardened oxygen-free copper (the data for the oxygen-free copper is taken from the literature [17]). The hardness of the Cu–Al_2O_3 composites slowly decreases with temperature without a sudden drop, resulting from the recovery, while recrystallization does not occur in the composites after annealing below 900 °C

[17]. However, the hardness curve of the oxygen-free copper suddenly drops in the 150–250 °C range, indicating recrystallization.

The measured yield and tensile strength of the cold-drawn Cu–Al_2O_3 bulk composites ($\varnothing$3 mm) is 417 MPa and 445 MPa, respectively. The tensile fracture morphology is shown in Fig. 7. The necking phenomenon is quite obvious in Fig. 7(a), and the reduction of the cross-sectional area reaches 80%. The macro-fracture presents the cup-cone morphology, which is typical for ductile fracture. The obvious circular axial interfacial crack in the center of the fracture surface in Fig. 7(b) indicates poor interfacial bonding in the center. The interface of the sheets at the center can be seen, with some slight intermittent small holes are seen in Fig. 7(c). There is less interface closer to the rim, which partially disappears.

The difference between the yield strength and the tensile strength is very small, resulting from the early necking occurring due to the internal defects, such as intermittent small holes.

To enhance the interfacial bonding and eliminate interfacial defects in the center, increasing the extrusion temperature or extrusion ratio may be needed.

4. Conclusions

(1) The hot extrusion rod contained Cu–Al_2O_3 bulk composites between 0.5 m and 3.9 m of the rod length. The center of the front portion of the hot extrusion rod was formed of the Cu–Al_2O_3 bulk composites, wrapped in a layer of packaging materials. The outside of the back portion was formed of the Cu–Al_2O_3 bulk composites with the packaging materials sandwich in the center. The electrical conductivity of the pure Cu–Al_2O_3 bulk composites in the extrusion rod was 96.3%IACS.

(2) After cold drawing, pure Cu–Al_2O_3 bulk composite wire with a diameter of 3 mm and a length of 84 m was obtained. The electrical conductivity of the composite wire was 94.1%IACS. The tensile strength was 445 MPa and the reduction of cross-sectional area reached 80%.

(3) After annealing below 900 °C, the hardness of the cold-drawn Cu–Al_2O_3 bulk composites decreased slowly with temperature, which indicated that the material has excellent resistance to high temperature annealing.

Acknowledgements

This study was supported by the National Natural Science Foundation of China (51201061), by the Plan for Scientific Innovation Talent of the Henan Province (144200510009), by the Henan Province Key Problem Project (092102210012), the Program for Changjiang Scholars and Innovative Research Team in University (IRT1234) and the program for Basic and Frontier Technologies Research in Henan Province (112300410002).

References

[1] D.W. Lee, G.H. Ha, B.K. Kim, Synthesis of Cu–Al_2O_3 nano composite powder, Scr. Mater. 44 (2001) 2137–2140.

[2] C. Biselli, D.G. Morris, Mechanical alloying of high-strength copper alloys containing TiB_2 and Al_2O_3 dispersoid particles, Scr. Metall. Mater. 30 (1994) 1327–1332.

[3] Meslet Al-Hajri, Aldo Melendez, R. Woods, T.S. Srivatsan, Influence of heat treatment on tensile response of an oxide dispersion strengthened copper, J. Alloys Comp. 290 (1999) 290–297.

[4] B.H. Tian, P. Liu, K.X. Song, Y. Li, Y. Liu, F.Z. Ren, J.H. Su, Microstructure and properties at elevated temperature of a nano-Al_2O_3 particles dispersion-strengthened copper base composite, Mater. Sci. Eng., A 435–436 (2006) 705–710.

[5] M.S. Motta, P.K. Jena, E.A. Brocchi, I.G. Solórzano, Characterization of Cu–Al_2O_3 nano-scale composites synthesized by in situ reduction, Mater. Sci. Eng., C 15 (2001) 175–177.

[6] Y.J. Li, F.Z. Ren, X.W. Wang, Y. Li, S.Z. Wei, Comparative study of internal oxidation microstructure of Cu–Al alloy with different Al content, Trans. Mater. Heat Treat. 35 (2014) 29–32 (in Chinese).

[7] R.H. Liu, K.X. Song, S.G. Jia, X.F. Xu, J.X. Gao, X.H. Guo, Morphology and frictional characteristics under electrical currents of Al_2O_3/Cu composites prepared by internal oxidation, Chin. J. Aeronaut. 21 (2008) 281–288.

[8] J. Grona, Heat-resistant dispersion-strengthened copper alloys, J. Mater. Eng. Perform. 1 (1992) 113–121.

[9] G.B. Li, J.B. Sun, Q.M. Guo, R. Wang, Fabrication of the nanometer Al_2O_3/Cu composite by internal oxidation, J. Mater. Process. Technol. 170 (2005) 336–340.

[10] K.X. Song, J.D. Xing, Q.M. Dong, P. Liu, B.H. Tian, X.J. Cao, Internal oxidation of dilute Cu–Al alloy powers with oxidant of Cu_2O, Mater. Sci. Eng., A 380 (2004) 117–122.

[11] S. Wood, D. Adamonis, A. Guha, W.A. Soffa, G.H. Meier, Internal oxidation of dilute Cu–Ti alloys, Metall. Trans. A 6 (1975) 1793–1800.

[12] F.F. Su, D.W. Zhang, D.M. Zhao, F.Z. Ren, B.H. Tian, S.G. Jia, Microstructure and properties of Cu–Al alloy sheet after internal oxidation, Trans. Mater. Heat Treat. 30 (2009) 101–104 (in Chinese).

[13] X.N. Zhang, D.W. Zhang, D.M. Zhao, P. Liu, F.Z. Ren, B.H. Tian, Study on microstructure of hot-extruded dispersion-strengthened Al_2O_3/Cu composite, Hot Work. Technol. 36 (2007) 7–9 (in Chinese).

[14] F.H. Scott, G.C. Wood, Internal oxidation, Mater. Sci. Technol. 4 (1988) 1072–1078.

[15] H.X. Li, B.H. Tian, Y.M. Lin, S.K. Li, P. Liu, Recrystallization behavior of Al_2O_3/Cu composite produced by internal oxidation, Rare Met. Mater. Eng. 34 (2005) 1039–1042 (in Chinese).

[16] F.Z. Ren, J. Wang, Z.H. Ma, J.H. Su, S.G. Jia, Properties of Cu and Fe under large deformation and strength calculation of Cu–115% Fe in situ composites, Trans. Mater. Heat Treat. 30 (2009) 17–21 (in Chinese).

[17] J.Y. Cheng, X.W. Ao, M.P. Wang, M.X. Guo, Effect of Al_2O_3 dispersed on microstructure of Cu–Al_2O_3 alloy annealed at elevated temperatures, Chin. J. Nonferr. Met. 19 (2009) 1928–1933 (in Chinese).